Proceedings of the 2004 International Conference
on Intelligent Mechatronics and Automation
Chengdu,China August 2004

Experimental Teleoperation of a Dual-Arm Manipulator Mounted on a Flexible Structure in Space

Dragomir N. Nenchev and Toshimitsu Hishinuma
Musashi Institute of Technology
1-28-1 Tamazutsumi, Setagaya-ku
Tokyo 158-8557, Japan
nenchev@sc.musashi-tech.ac.jp

Abstract— **This paper describes an experimental system for teleoperation of a dual-arm manipulator mounted on a flexible base. The manipulators and the base are arranged in the horizontal plane so that gravity forces can be neglected and a long-reach manipulator for space application is envisioned. Based on the Reaction Null Space concept developed previously, we propose several strategies for telecontrol of the dual-arm manipulator and verify their perfomance experimentally.**

I. Introduction

The concept of a so-called *macro-micro manipulator system* has been introduced by Sharon and Hardt [1] twenty years ago. A small manipulator was mounted on the end of a larger one, so that the former could be relocated to a remote place by means of the latter. Controlling the motion of a such a system is quite challenging due to the presence of structural deflections in the macro part and the existing dynamic coupling between the two substructures. Similar phenomena occur also in so-called *long-reach manipulators (LRM's)* comprising a rigid-arm manipulator mounted at the end of a long supporting beam. The macro-micro manipulator or LRM concept has evolved throughout the years to meet mainly two types of application demands: nuclear waste cleanup [2], [3] and space robotics [4], [5].

In our previous research we have developed a concept called the *Reaction Null Space* which was applied to motion planning and control of a single-arm LRM [6] and a dual-arm LRM [7]. Via the reaction null space, we decomposed the joint space such that dynamic decoupling between the macro and the micro subsystems is achieved. Thus, it was possible to suppress vibrations in the macro part in an efficient way, and also, to generate reactionless motions.

Our research so far has focused on the execution of preplanned trajectories. It should be apparent, though, that in practice, a major mode of operation of a LRM for space application would be teleoperation. It is, therefore, necessary to study the behavior of LRM's within the framework of teleoperation. The aim of this work is to propose several strategies for teleoperation of single- and dual-arm LRM's under zero gravity and to verify the performance with experiments.

II. Notation and Background

A. Equation of Motion of a Long Reach Manipulator

We consider a dual-arm LRM; the general case of a multi-arm LRM is easily derivable from the model below. We will refer to the two arms as "upper" and "lower" arm, and use subscripts u and l in the notation. For example, the number of joints will be denoted as n_u and n_l, respectively. The *system dynamics* can be written in the following form [6], [7]:

$$\begin{bmatrix} \boldsymbol{H}_b(\boldsymbol{x}_b,\boldsymbol{\theta}) & \boldsymbol{H}_{bm}(\boldsymbol{x}_b,\boldsymbol{\theta}) \\ \boldsymbol{H}_{bm}^T(\boldsymbol{x}_b,\boldsymbol{\theta}) & \boldsymbol{H}_m(\boldsymbol{x}_b,\boldsymbol{\theta}) \end{bmatrix} \begin{bmatrix} \ddot{\boldsymbol{x}}_b \\ \ddot{\boldsymbol{\theta}} \end{bmatrix} + \begin{bmatrix} \boldsymbol{D}_b\dot{\boldsymbol{x}}_b \\ \boldsymbol{0} \end{bmatrix} + \begin{bmatrix} \boldsymbol{K}_b\boldsymbol{x}_b \\ \boldsymbol{0} \end{bmatrix} + \begin{bmatrix} \boldsymbol{c}_b(\boldsymbol{x}_b,\dot{\boldsymbol{x}}_b,\boldsymbol{\theta},\dot{\boldsymbol{\theta}}) \\ \boldsymbol{c}_m(\boldsymbol{x}_b,\dot{\boldsymbol{x}}_b,\boldsymbol{\theta},\dot{\boldsymbol{\theta}}) \end{bmatrix} = \begin{bmatrix} \boldsymbol{0} \\ \boldsymbol{\tau} \end{bmatrix}, \quad (1)$$

where $\boldsymbol{x}_b \in \Re^m$ denotes the positional and orientational deflection of the base with respect to the inertial frame[1] , $\boldsymbol{\theta} \in \Re^n (n = n_u + n_l)$ stands for the generalized coordinates of the two arms, $\boldsymbol{H}_b$, $\boldsymbol{D}_b$ and $\boldsymbol{K}_b \in \Re^{m\times m}$ denote base inertia, damping and stiffness, respectively. $\boldsymbol{H}_m \in \Re^{n\times n}$ is the block-diagonal inertia matrix of the two arms. $\boldsymbol{H}_{bm} \in \Re^{m\times n}$ denotes the so-called *inertia coupling matrix*. $\boldsymbol{c}_b$ and $\boldsymbol{c}_m$ are velocity-dependent nonlinear terms, and $\boldsymbol{\tau} \in \Re^n$ is the joint torque. We do not consider external forces here, including gravity forces, since we focus only on noncontact tasks in micro gravity environment.

We focus on two main control subtasks: (1) active vibration suppression at a point where the arms are stationary, and (2) initializing motion such that no vibrations in the base occur.

B. The Vibration Suppression Control Subtask

The vibration suppression control subtask has been solved by Lee and Book [8] based on the singular perturbation technique. Another possible approach is that of Konno and Uchiyama used for active vibration suppression of a flexible-link manipulator [9]. The essential assumptions in this case are two: (1) since the arm is stationary at the initial instant, the nonlinear velocity-dependent terms $\boldsymbol{c}_b$ and $\boldsymbol{c}_m$ are approximated with zero, and (2) the deflections are assumed small, and hence, all inertia submatrices are approximated to be functions of the joint variables only. Note that also in the case of a LRM, these two assumptions are

[1] Generally, $m = 6$ $(n \geq m)$.

0-7803-8748-1/04/$20.00 ©2004 IEEE.

sufficient to cancel all velocity-dependent terms, including those which do not include the joint velocity explicitly (i.e. $\dot{\boldsymbol{H}}_b(\boldsymbol{\theta})\dot{\boldsymbol{x}}_b$, $\dot{\boldsymbol{H}}^T_{bm}(\boldsymbol{\theta})\dot{\boldsymbol{x}}_b$). Then, the upper part of the equation of motion can be linearized around the equilibrium of the base:

$$\boldsymbol{H}_b\ddot{\boldsymbol{x}}_b + \boldsymbol{D}_b\dot{\boldsymbol{x}}_b + \boldsymbol{K}_b\boldsymbol{x}_b = -\boldsymbol{H}_{bm}\ddot{\boldsymbol{\theta}}. \tag{2}$$

Choose the control acceleration as

$$\ddot{\boldsymbol{\theta}}_b = \boldsymbol{H}^+_{bm}\boldsymbol{G}_b\dot{\boldsymbol{x}}_b, \tag{3}$$

where $\boldsymbol{G}_b$ is a gain matrix, and $\boldsymbol{H}^+_{bm} \in \Re^{n\times m}$ denotes the Moore-Penrose generalized inverse of the inertia coupling matrix. Then, since $\boldsymbol{H}_{bm}\boldsymbol{H}^+_{bm} = \boldsymbol{E}$, $\boldsymbol{E}$ denoting the unit matrix of proper dimension, it is easy to verify that the damping of the base will increase from $\boldsymbol{D}_b$ to $\boldsymbol{D}_b + \boldsymbol{G}_b$.

C. Reactionless Motion Control Subtask

At $t = t_0$ we assume a stationary base. Then, we look for motions in the macro part which would maintain the zero state of the base. Of course, in this case too, we can assume all inertia submatrices to be functions of the joint variables only. In addition, all nonlinear velocity-dependent terms contributed by the base deflection rate $\dot{\boldsymbol{x}}_b$ will be zero.

With a stationary base as initial condition, the base reaction wrench $\mathcal{F}_0 = \mathcal{F}(t_0)$ due to motion of the arm can be written as:

$$\mathcal{F}_0 = \frac{d}{dt}\begin{bmatrix} w\dot{\boldsymbol{r}}_{cm} \\ \boldsymbol{r}_{cm}\times w\dot{\boldsymbol{r}}_{cm} + \sum_{j=1}^{n}(\boldsymbol{I}_j\boldsymbol{\omega}_j + \boldsymbol{r}_j \times m_j\dot{\boldsymbol{r}}_j) \end{bmatrix}, \tag{4}$$

where $\boldsymbol{r}_{cm}$ denotes the total center of mass of the arm, $\boldsymbol{I}_j$, $\boldsymbol{\omega}_j$, m_j, $\boldsymbol{r}_j$ stand for the inertia matrix, angular velocity, mass and center-of-mass position for link j, respectively, and $w = \sum m_j$. The base reaction can be rewritten in terms of arm joint variables, as follows:

$$\mathcal{F}_0 = \boldsymbol{H}_{bm}\ddot{\boldsymbol{\theta}} + \dot{\boldsymbol{H}}_{bm}\dot{\boldsymbol{\theta}}. \tag{5}$$

The state of stationary base will be maintained under a manipulator control law, if it exists, such that $\mathcal{F}(t) = \boldsymbol{0}$ for all $t \geq t_0$. In this case, base equilibrium is

$$\boldsymbol{H}_b\ddot{\boldsymbol{x}}_b + \boldsymbol{D}_b\dot{\boldsymbol{x}}_b + \boldsymbol{K}_b\boldsymbol{x}_b = \boldsymbol{0} = -\boldsymbol{H}_{bm}\ddot{\boldsymbol{\theta}} - \dot{\boldsymbol{H}}_{bm}\dot{\boldsymbol{\theta}}. \tag{6}$$

The specific motion of the manipulator that maintains base equilibrium, i.e.

$$\boldsymbol{H}_{bm}\ddot{\boldsymbol{\theta}} + \dot{\boldsymbol{H}}_{bm}\dot{\boldsymbol{\theta}} = \boldsymbol{0} \tag{7}$$

we call *reactionless manipulator motion*. The above equation can be integrated to:

$$\mathcal{L}(t) = \mathcal{L}_0 + \boldsymbol{H}_{bm}\dot{\boldsymbol{\theta}}(t),\ t \geq t_0, \tag{8}$$

where $\mathcal{L}_0 = \mathcal{L}(t_0) = \boldsymbol{H}_{bm}\dot{\boldsymbol{\theta}}(t_0)$ is the integration constant. This integral we call *the coupling momentum*.

From Equations (5) and (8) it is apparent that the arms will not induce any reaction to the base if and only if the coupling momentum is conserved ($\mathcal{L} = \text{const} \Leftrightarrow \mathcal{F} = \boldsymbol{0}$).

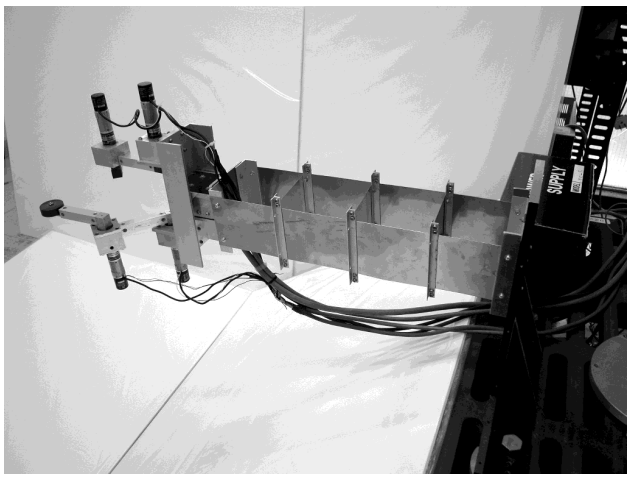

Fig. 1. The experimental LRM system.

Let us assume that $n > m$ holds. Then, solving Equations (5) and (8) under the above conditions, we obtain:

$$\ddot{\boldsymbol{\theta}}_c = -\boldsymbol{H}^+_{bm}\dot{\boldsymbol{H}}_{bm}\dot{\boldsymbol{\theta}} + (\boldsymbol{E} - \boldsymbol{H}^+_{bm}\boldsymbol{H}_{bm})\boldsymbol{\zeta} \tag{9}$$

and

$$\dot{\boldsymbol{\theta}}_c = \boldsymbol{H}^+_{bm}\mathcal{L}_0 + (\boldsymbol{x}_b - \boldsymbol{H}^+_{bm}\boldsymbol{H}_{bm})\boldsymbol{\zeta} \tag{10}$$

for joint acceleration and joint velocity, respectively. The expression $\boldsymbol{P}_{RNS} \equiv (\boldsymbol{E} - \boldsymbol{H}^+_{bm}\boldsymbol{H}_{bm})$ denotes a projector onto the null space of the inertia coupling matrix and $\boldsymbol{\zeta} \in \Re^n$ is arbitrary. The null space we call *the reaction null-space*.

The reaction null space exists whenever the condition $n > m$ is met. Equation (9) shows that the arms can accelerate within this null space, from rest, without disturbing the base equilibrium. The zero initial coupling momentum will be then necessarily conserved. Of course, it would be necessary to consider only practically meaningful motion within the set of all reactionless motion. A practically meaningful motion is determined from a specific end-effector motion task. Such a task would impose an additional constraint onto the system, and hence, decrease the number of effective degrees of freedom. We will consider the two typical cases of single-arm operation and dual arm-operation. In the former case, one of the arms is totally free: all its degrees of freedom can be used to constitute the reaction null space. In the latter case, however, this is not so: the reaction null space shrinks significantly and may even disappear.

III. The Experimental LRM System

Our experimental LRM is depicted in Figure 1. It consists of two small planar 2R rigid link manipulators attached to the free end of a flexible double beam representing the flexible base. Due to the specific design, we can assume that the base deflects only from the longitudinal axis. In other words, the reaction moment and the reaction force component along the longitudinal axis of the base can be neglected as a disturbance.

The control architecture is shown in Figure 2. The deflection of the flexible base is measured by a strain gauge.

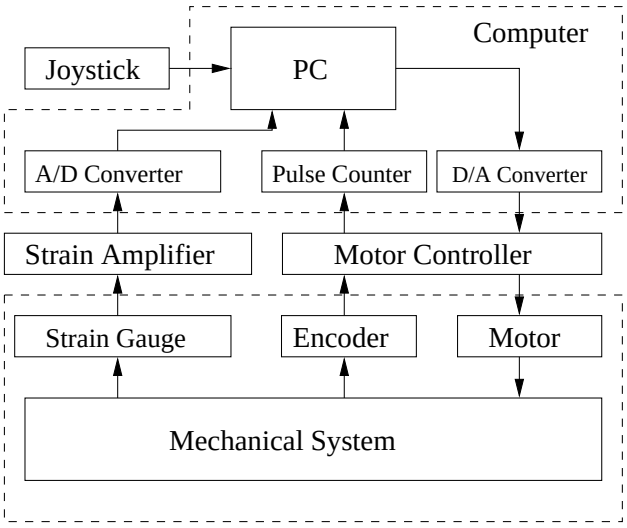

Fig. 2. Control architecture of the experimental LRM system.

The strain gauge signal is used for feedback base deflection control, i.e. in the case of vibration suppression. A joystick is connected to the control PC to generate end-effector commands for one of the manipulator arms (the lower arm). The motor controller works in velocity control mode.

The system model is depicted in Figure 3. The parameters of one of the arms (the two are identical) and the base parameters are presented in Tables I and II, respectively. The natural frequency, damping ratio and base siffness were estimated using the logarithmic decrement method applied to damped free vibration experimental data. The values obtained for the natural frequency and the damping ratio are: $\omega_n = 9.67$ rad/s and $\zeta = 0.035$.

TABLE I
Manipulator link parameters

l_1	0.1	[m]
l_2	0.1	[m]
l_{g1}	0.05	[m]
l_{g2}	0.05	[m]
m_1	0.025	[kg]
m_2	0.285	[kg]
m_3	0.025	[kg]
m_4	0.095	[kg]
I_1	1.35×10^{-2}	[kgm^2]
I_2	3.07×10^{-3}	[kgm^2]

As already explained, we consider just the reaction force component along the low stiffness direction (the x axis of the elastic-base coordinate frame). This means that $m = 1$. Since each arm has two motors ($n = 4$), the reaction null space is three-dimensional.

To derive the reaction null space, we need the inertia coupling matrix. In our case $\boldsymbol{H}_{bm}$ is 3×4. Since we are interested in the reaction force only along the low-stiffness x axis, we will apply the selective reaction null space procedure [6]. Essentially, this will reduce dimension by two, taking only the first row of $\boldsymbol{H}_{bm}$, which corresponds exactly to that reaction force. Denote the reduced inertia coupling matrix as

TABLE II
Flexible base parameters

Length	0.4	[m]
Height	0.1	[m]
Width	0.09	[m]
Thickness	1×10^{-3}	[m]
Tip mass $H_b(\equiv m_0)$	2.37	[kg]
Stiffness K_b	230	[N/m]
Damping D_b	1.35	[Ns/m]

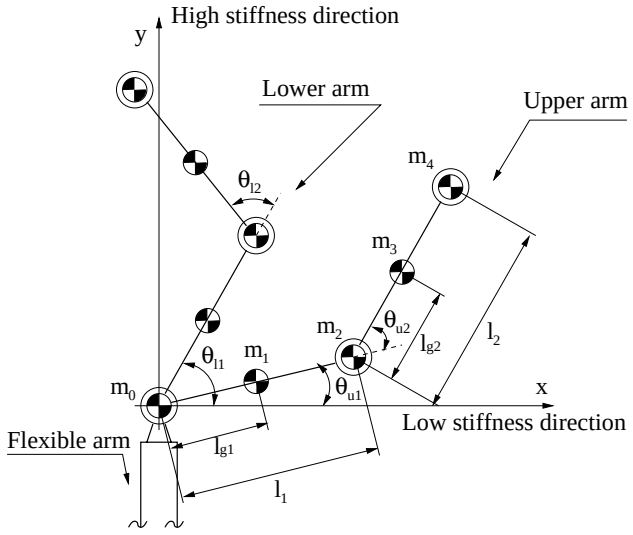

Fig. 3. A model of the experimental LRM system.

$$\hat{\boldsymbol{H}}_{bm} = \begin{bmatrix} \hat{\boldsymbol{H}}_{bmu} & \hat{\boldsymbol{H}}_{bml} \end{bmatrix} \tag{11}$$

where $\hat{\boldsymbol{H}}_{bmu}$ and $\hat{\boldsymbol{H}}_{bml}$ are 1×2 components denoting inertial coupling for the low-stiffness axis due to the upper and lower arm, respectively. Now we can write the coupling momentum equation as

$$\hat{\boldsymbol{H}}_{bmu}\dot{\boldsymbol{\theta}}_u + \hat{\boldsymbol{H}}_{bml}\dot{\boldsymbol{\theta}}_l = \mathcal{L} \tag{12}$$

where $\boldsymbol{\theta}_u$ and $\boldsymbol{\theta}_l$ are two-dimensional joint variable vectors of the upper and the lower arm, respectively. Note that if the x motion component of the centroid of the two arms is denoted as r_c^x, then $\mathcal{L} = wr_c^x$ where w is the total mass of the arms.

IV. A Single-Arm LRM Teleoperation Strategy

A representative of a single-arm LRM for space application is the manipulator system on the Japanese Experimental Module which will be connected to the International Space Station in the near future. The manipulator system comprises a large six-DOF manipulator arm ensuring access within a wide workspace, and a small six-DOF arm for dexterous operation. Once relocated, the large arm can be

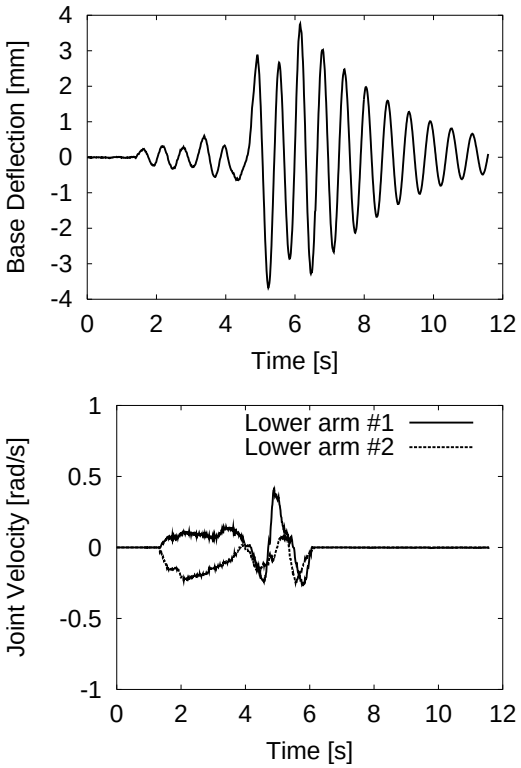

Fig. 4. Single-arm teleoperation without vibration suppression.

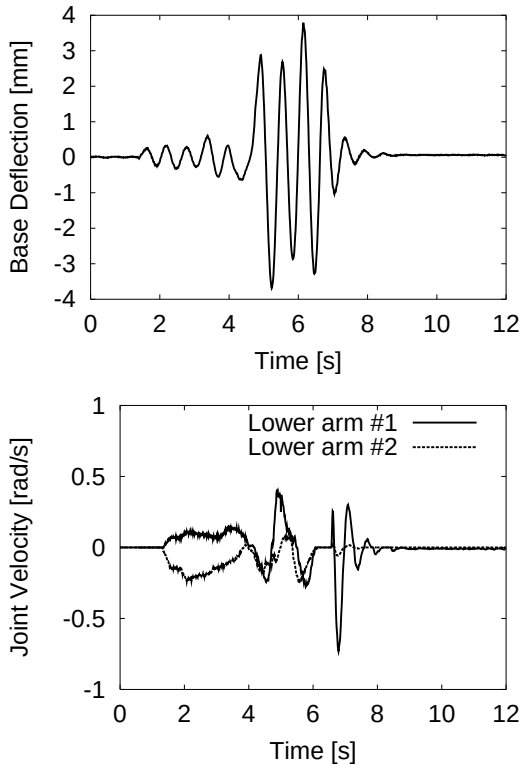

Fig. 5. Single-arm teleoperation with vibration suppression.

considered as a flexible passive base for the small arm. The number of DOF's of the small arm are equal to that of the base, and hence, the reaction null space will consist of the zero vector only. This means that no reactionless motions can be generated. A reasonable strategy would be then to employ the vibration suppression technique via the small arm, after its commanded motion has finished.

We will demonstrate this technique with our experimental LRM. The joystick command is used to control the end-effector motion of the lower arm in velocity mode. Because the motor controller works in such mode, we need to obtain the joint velocity by integrating Eq. (3). Now, it is reasonable to assume that the inertia coupling matrix $\boldsymbol{H}_{bml}$ is constant since base deflection is assumed small and hence, the joint angles will not change much. Thus, we can simplify the integration and apply the following velocity-based control law:

$$\dot{\boldsymbol{\theta}}_b = \bar{\boldsymbol{H}}^{+}_{bml} \boldsymbol{G}_b \boldsymbol{x}_b \tag{13}$$

where $\bar{\boldsymbol{H}}_{bml} = \boldsymbol{H}_{bml}(\boldsymbol{\theta} = \text{const})$.

Based on the above vibration suppression control law, experiments on teleoperation with vibration suppression have been conducted. Since the small arm has two DOFs and the flexible base just one, the inertia coupling matrix $\boldsymbol{H}_{bml}$ is 1 by 2. In the experiment, vibration suppression was initialized by the operator after she completed the commanded motion. This means that the constant $\bar{\boldsymbol{H}}_{bml}$ was evaluated with the final joint configuration attained.

First, we conducted a teleoperation experiment without vibration suppression. Figure 4 shows base deflection and joint velocity data. In the beginning ($0 < t < 4$ s) a slow motion command was given. We obtained a low-amplitude vibration of the base, accordingly. Then, the operator commanded a higher-velocity motion in combination with changes in the motion direction. Consequently, the base began to vibrate significantly. Due to the low structural damping, vibration continued for a relatively long period after the motion of the small arm motion was completed.

Next, a teleoperation experiment with vibration suppression was performed. In order to ensure comparability, input data recorded during the previous experiment was used. Figure 5 shows base deflection and joint velocity data. The vibration suppression control was activated shortly after the base began to vibrate with high amplitude, around $t = 6.5$ s. The vibration was suppressed within two periods after this, which demonstrates the efficiency of the vibration suppression law.

V. Two Dual-Arm LRM Teleoperation Strategies

The lower arm end-point velocity is commanded via the joystick. The upper arm will be used to cancel the induced reaction force in the base. Indeed, consider Eq. (12) with the initial momentum assumed zero. It should be apparent then that the reactions of both arms cancel out if the following holds:

$$\hat{\boldsymbol{H}}_{bmu} \dot{\boldsymbol{\theta}}_u = -\hat{\boldsymbol{H}}_{bml} \dot{\boldsymbol{\theta}}_l. \tag{14}$$

Based on the above equation, we will consider two compensation strategies:

- symmetrical motion;
- asymmetrical motion.

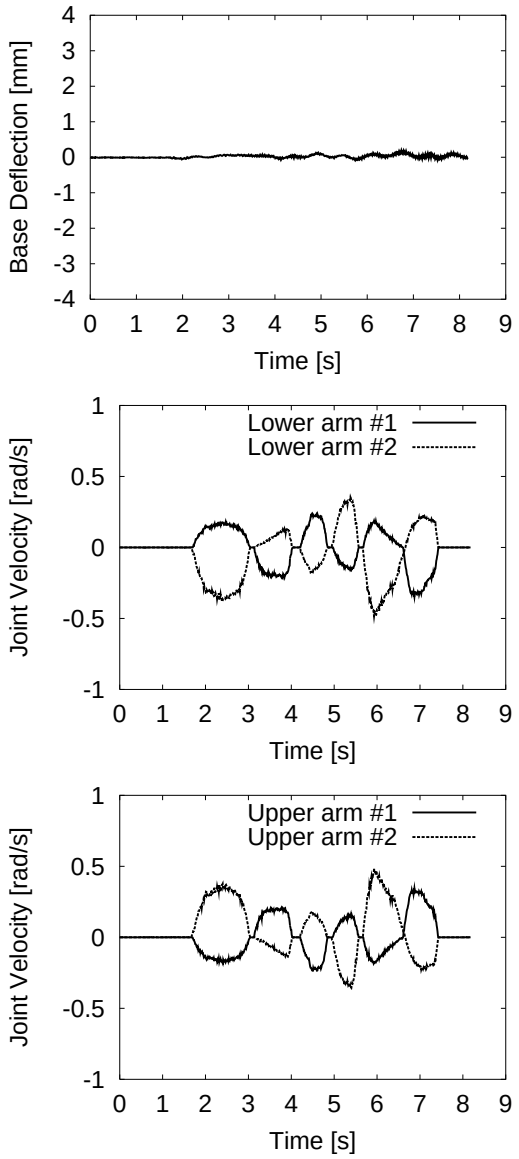

Fig. 6. Reactionless teleoperation with symmetrical motion.

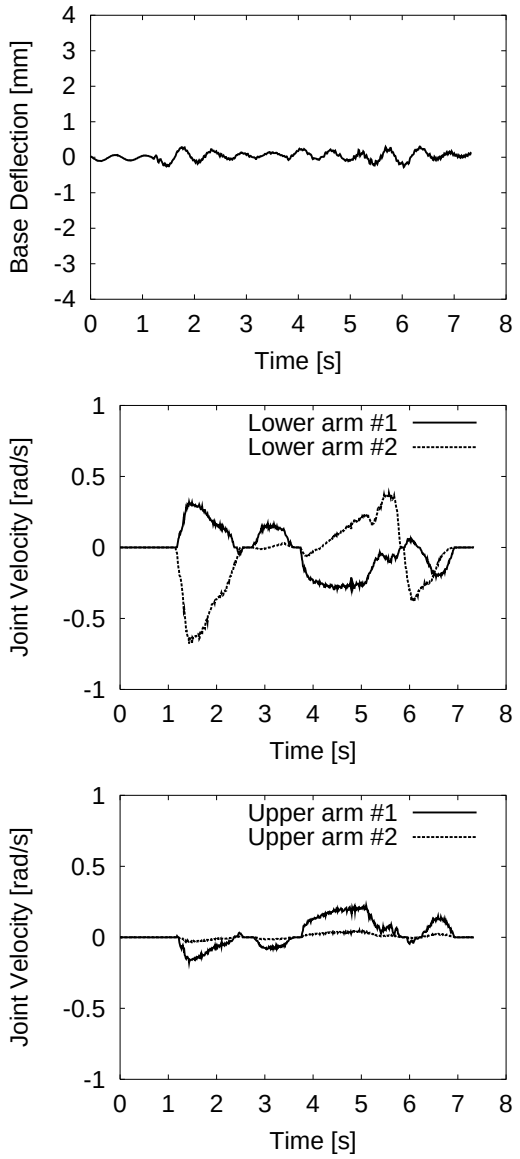

Fig. 7. Reactionless teleoperation with asymmetrical motion.

A. Symmetrical motion

The simplest way to enforce Eq. (14) is to employ a "mirroring" motion for the two arms, under the assumption of a symmetrical initial configuration w.r.t. the y axis, i.e.:

$$\theta_{l1} = \pi/2 \pm \alpha \Rightarrow \theta_{u1} = \pi/2 \mp \alpha$$

and

$$\theta_{l2} = \pm\beta \Rightarrow \theta_{u2} = \mp\beta.$$

Then, the "mirroring" joint velocity of the upper arm is simply:

$$\dot{\boldsymbol{\theta}}_u = -\dot{\boldsymbol{\theta}}_l. \tag{15}$$

We call this strategy "symmetrical motion" strategy.

A teleoperation experiment was conducted with symmetrical motion. The initial configuration for both arms was $[\pi/2, 0]$ rad. Figure 6 shows the experimental data. It is seen that the induced base vibration amplitude is of very low order, less than 0.3 mm.

B. Asymmetrical motion

A symmetrical initial arm configuration might not always be available in practice. Another way to enforce Eq. (14) is to solve it for $\dot{\boldsymbol{\theta}}_u$:

$$\dot{\boldsymbol{\theta}}_u = -\hat{\boldsymbol{H}}^{+}_{bmu}\hat{\boldsymbol{H}}_{bml}\dot{\boldsymbol{\theta}}_l + (\boldsymbol{E} - \hat{\boldsymbol{H}}^{+}_{bmu}\hat{\boldsymbol{H}}_{bmu})\boldsymbol{\zeta}. \tag{16}$$

The pseudoinverse of the upper-arm inertia coupling matrix has to be used because $\hat{\boldsymbol{H}}_{bmu}$ is 1 by 2. The expression $(\boldsymbol{E} - \hat{\boldsymbol{H}}^{+}_{bmu}\hat{\boldsymbol{H}}_{bmu})$ denotes a projector onto the null space of the upper-arm inertia coupling matrix. Joint velocity from this null space does not contribute to the base reaction generated by the upper arm. Hence, the arbitrary vector $\boldsymbol{\zeta}$ can be simply set to zero.

A teleoperation experiment with asymmetrical motion was conducted. The initial configuration for both arms was again $[\pi/2, 0]$ rad. Figure 7 shows the experimental data. It is seen that the induced base vibration amplitude

is a little bit higher than that of symmetrical motion, but still the order is much lower as compared to the case of single-arm teleoperation where no reaction compensation was available at all. Note that the pseudoinverse solution minimizes the joint velocity norm. Indeed, from the upper-arm velocity graph it can be inferred that the reaction is compensated with a relatively low joint velocity. If the arbitrary vector ζ in Eq. (16) is chosen to be nonzero, other asymmetrical motion strategies can be obtained, this goes however beyond the scope of the paper.

VI. Conclusions

This work has shown how the reaction null space concept can be applied to a LRM system within a teleoperation framework. First, we have introduced a possible strategy for teleoperating a nonredundant single-arm LRM without capability of reaction compensation. This strategy makes use of the efficient vibration suppression control law proposed in our previous study. Experiments have confirmed the results.

Next, we introduced two strategies for teleoperation of a dual-arm LRM system, where one of the arms is teleoperated directly, while the other arm is compensating the reaction. These strategies were confirmed also successfully by experiments. One of the strategies, called "asymmetrical," is efficient in the sense that a minimum-norm solution for the compemsating joint velocity was obtained.

Finally, it should be mentioned that the experimental results have been derived with a relatively simple planar system, but the theoretical base developed covers the general case of a spatial LRM.

References

[1] A. Sharon and D. Hardt, "Enhancement of robot accuracy using end-point feedback and a macro-micro manipulator system," in Proc. ACC, San Diego, CA, 1984, pp. 1836–1842.

[2] J. F. Jansen et al., "Long-reach manipulation for waste storage tank remediation," DSC–Vol. 31, ASME, pp. 67–73, 1991.

[3] D.-S. Kwon et al., "Input shaping filter methods for the control of structurally flexible, long-reach manipulators," in Proc. IEEE Int. Conf. Robotics and Automation, San Diego, CA, 1994, pp. 3259–3264.

[4] M. A. Torres and S. Dubowsky, "Path-planning in elastically constrained space manipulator systems," in Proc. IEEE Int. Conf. Robotics and Automation, Atlanta, Georgia, 1993, pp. 812–817.

[5] C. Vallancourt and C. M. Gosselin, "Compensating for the structural flexibility of the SSRMS with the SPDM," 2nd Workshop on Robotics in Space, Canadian Space Agency, Montreal, Canada, July 1994.

[6] D. N. Nenchev, K. Yoshida, P. Vichitkulsawat and M. Uchiyama, "Reaction null-space control of flexible structure mounted manipulator systems," IEEE Tr. on Robotics and Automation, Vol. 15, No. 6, pp. 1011–1023, December 1999.

[7] Akio Gouo, Dragomir N. Nenchev, Kazuya Yoshida, Masaru Uchiyama, "Motion Control of Dual-Arm Long-Reach Manipulators," Advanced Robotics, Vol. 13, No. 6, pp. 617–632, 2000.

[8] S. H. Lee and W. J. Book, "Robot vibration control using inertial damping forces," in Proc. of the Eight CISM–IFToMM Symp. RoManSy 8, Cracow, Poland, 1990, pp. 252–259.

[9] M. Uchiyama, and A. Konno, "Modeling, controllability and vibration suppression of 3D flexible robots," Robotics Research: The Seventh International Symposium, Ed. by G. Giralt and G. Hirzinger, Springer Verlag, 1996, pp. 90–99.